Optics & Laser Technology 188 (2025) 112954

Contents lists available at ScienceDirect

Optics and Laser Technology

journal homepage: www.elsevier.com/locate/optlastec

Full length article

# Visible actively mode-locked fiber lasers at 635/602/546 nm☆

Tianran Li [a,b], Shuo Zhang [a], Jinliang Yuan [a], Yikun Bu [a], Mingjia Shangguan [c,*], Zhengqian Luo [a,b,*]

[a] Fujian Key Laboratory of Ultrafast Laser Technology and Applications, Xiamen University, Xiamen, 361005, Fujian, China
[b] Shenzhen Research Institute of Xiamen University, Xiamen University, Shenzhen, 518129, Guangdong, China
[c] State Key Laboratory of Marine Environmental Science, College of Ocean and Earth Sciences, Xiamen University, Xiamen, 361102, Fujian, China

ARTICLE INFO

*Keywords:*
Actively mode-locking
Visible fiber laser
Acousto-optic modulator

ABSTRACT

An actively mode-locked (AML) fiber laser is widely applied in fields such as optical communication, optical frequency comb, and broadband signal processing due to its advantages of simple structure, good controllability, and easy integration. However, the development of visible AML fiber lasers has stagnated due to the immaturity of visible devices and the challenges in splicing visible fluoride gain fibers. In this work, we demonstrate the direct generation of AML pulses at red (635 nm), orange (602 nm), and green (546 nm) wavelengths in rare earth ion-doped fluoride fiber lasers using an acousto-optic modulator (AOM). For the first time, we obtained orange and green AML pulses with average powers of 11 mW and 102 mW, respectively, while achieving a red AML pulse with an average power of 275 mW, representing a two-order-of-magnitude improvement over previous results. The narrowest mode-locked pulse widths for red, orange, and green wavelengths are 448 ps, 12 ns, and 19 ns, respectively, at repetition frequencies of 8.56 MHz, 1.25 MHz, and 4.06 MHz. This work is an important step in applying AML technology to fiber lasers covering the visible spectral region.

## 1. Introduction

Visible ultrafast lasers, as ideal light sources for a variety of cutting-edge scientific research, have received extensive attention from researchers in recent years [1–4]. The conventional method for generating visible ultrashort pulses is nonlinear frequency conversion technology [5–7], including optical parametric oscillators and amplifiers, frequency doubling, sum-frequency generation, and Cherenkov radiation. In contrast, mode-locked rare-earth fiber lasers, with their advantages of low cost, excellent performance, good flexibility, and compact structure, enable the direct generation of visible ultrashort pulses and are regarded as a novel and promising technology. In the past few decades, the development of compact mode-locked fiber lasers in the visible wavelength region has been a significant focus in laser technology.

The core technologies of visible mode-locked fiber lasers mainly include two categories: passive mode-locking and active mode-locking. Currently, visible fiber lasers primarily generate laser emission by pumping rare-earth-doped $ZrF_4$–$BaF_2$–$LaF_3$–$AlF_3$–NaF (ZBLAN) fibers with laser diodes (LDs). Among them, various research achievements related to passively mode-locked fiber lasers based on nonlinear polarization evolution (NPE) and nonlinear optical loop mirrors (NOLMs) have been frequently reported [8–16]. In 2018, Zou et al. successfully developed a 96 ps $Pr^{3+}$ fluorine-doped fiber laser with NOLM mode-locking at 635 nm [8]. Subsequently, Luo et al. used nonlinear polarization rotation (NPR) technology to obtain yellow mode-locked pulses in $Dy^{3+}$: ZBLAN fiber, with the narrowest pulse width reaching 83 ps [9]. They also used artificial intelligence technology to assist in exploring the optimal mode-locked polarization state of green light in $Ho^{3+}$: ZBLAN fiber, thereby obtaining green mode-locked pulses of 27.9 ps [10]. In 2023, Marie-Pier Lord et al. and Zou et al. used NPR and phase-biased nonlinear amplifying loop mirror (PB-NALM), respectively, to successfully obtain femtosecond mode-locked pulses at 635 nm [11,13]. Researchers have recognized that these passive mode-locking schemes can obtain high-performance mode-locked pulses in multiple visible wavelengths through a universal structure. However, the passive mode-locking scheme is difficult to control externally and is highly susceptible to environmental influences. Thus, alternative solutions are often needed in some research and applications of ultrafast lasers.

☆ This work was supported by the National Natural Science Foundation of China (62235014, 62022069, 62305275), and Shenzhen Science and Technology Projects, China (JCYJ20210324115813037).

* Corresponding authors.
*E-mail addresses:* 23120210155968@stu.xmu.edu.cn (T. Li), shuozhang@stu.xmu.edu.cn (S. Zhang), yuanjinliang@stu.xmu.edu.cn (J. Yuan), buyikun0522@xmu.edu.cn (Y. Bu), mingjia@xmu.edu.cn (M. Shangguan), zqluo@xmu.edu.cn (Z. Luo).

https://doi.org/10.1016/j.optlastec.2025.112954
Received 15 September 2024; Received in revised form 24 March 2025; Accepted 8 April 2025
Available online 23 April 2025

Unlike passive mode-locking, which relies on adjusting the polarization state in the cavity, active mode-locking is an alternative technology that generates laser pulses by applying intensity or phase modulation to match the frequency with the cavity length [17–19]. The switch for active mode-locking operation is controlled by external electrical signals, resulting in a mode-locking state with high resistance to interference and excellent self-starting characteristics [20–22]. Due to the simple structure and low cost of active mode-locked fiber lasers, they have become commercial light sources in various applications. Since researchers first observed unstable mode-locking and Q-switching states at 650 nm in 1990, active mode-locking in the visible spectrum has remained an active area of research. In 2000, the first report on visible mode-locked fiber lasers was published, which utilized a fiber phase modulator to generate an active mode-locked pulse of 550 ps in $Pr^{3+}/Yb^{3+}$-doped ZBLAN fiber at 635 nm [23]. However, because this fiber phase modulator is matched to the few-mode $Pr^{3+}/Yb^{3+}$-doped ZBLAN fiber (with core and cladding diameters of 3.5 μm and 125 μm, respectively, and a numerical aperture of 0.16), the output power of this laser is only 3 mW. To the best of our knowledge, no reports indicate that this fiber phase modulator is suitable for visible gain fibers with large core diameters (such as $Ho^{3+}$: ZBLAN fiber and $Dy^{3+}$: ZBLAN fiber) to generate other visible wavelengths, driving researchers to seek a universal alternative. In recent years, the continuous development of visible gain fibers and modulators has provided strong support for active mode-locking schemes. For example, double-clad $Pr^{3+}$: ZBLAN fiber, which supports high-power operation, and novel acousto-optic modulators (AOMs) in the visible spectrum have laid a solid foundation for AML operation in visible wavelengths [24–27]. Since the 21st century, the development of visible AML fiber lasers has experienced significant stagnation. Therefore, addressing this long-standing challenge has become a highly significant and passionate scientific pursuit.

In this paper, we propose and present three types of visible actively mode-locked fiber lasers in red (635 nm), orange (602 nm), and green (546 nm). Firstly, the gain fibers we selected are double-clad $Pr^{3+}$-doped ZBLAN fiber, $Pr^{3+}/Yb^{3+}$-doped ZBLAN fiber, and $Ho^{3+}$-doped ZBLAN fiber, as they exhibit strong gain capabilities at red, orange, and green wavelengths, respectively. Subsequently, we utilize self-made fiber dielectric mirrors (FDMs) and plane mirrors to construct the resonators for red, orange, and green lights. Finally, we achieve active mode-locking operation by inserting a spatial acousto-optic modulator (AOM) for intensity modulation. The Gaussian actively mode-locked pulses with central wavelengths of 635 nm/602 nm/546 nm have spectral bandwidths of 2.12 nm/0.42 nm/1.02 nm and pulse durations of 448 ps/12 ns/19 ns, respectively. The stable mode-locking operation has signal-to-noise ratios (SNRs) of 61 dB/63 dB/48 dB and repetition rates of 8.56 MHz/1.56 MHz/4.06 MHz, respectively. Additionally, we measured the beam quality and output powers (275 mW, 11 mW, 102 mW) of the three actively mode-locked fiber lasers in red, orange, and green. Among them, the actively mode-locked fiber lasers in orange and green wavelengths are reported for the first time, and the output power of the red actively mode-locked fiber laser is enhanced by approximately two orders of magnitude compared to previous works. Compared with the relatively mature passive mode-locked visible fiber laser technology, this work represents a novel paradigm that is simple, active, and maneuverable, with multiple potential applications. This indicates that the AML technology with AOM as the core can be applied to various visible wavelengths and has numerous potential development possibilities.

## 2. Experimental setup

Fig. 1(a, c, e) presents the experimental setups of the AML laser at 635 nm/602 nm/546 nm, while Fig. 1(b, d, f) presents the corresponding photographs. As depicted in Fig. 1(a), the red laser consists of a 443 nm diode laser, a 10 m double-clad $Pr^{3+}$-doped ZBLAN fiber as the gain fiber, and a red highly reflective FDM ($M_1$). A dichroic mirror ($M_2$) forms a red resonator, along with a free-space AOM serving as the active mode-locking switch. The double-clad (DC) $Pr^{3+}$-doped fluoride fiber, manufactured by Le Verre Fluoré, has the following attributes: a core diameter of 7.5 μm, a double D-shaped inner-clad profile with dimensions of 115 μm by 125 μm, and an outer cladding diameter of 180 μm [28]. Additionally, it has an inner-clad NA of 0.45, a core numerical aperture (NA) of 0.08, and a $Pr^{3+}$ doping concentration of 8000 ppm (wt.). The FDM ($M_1$) connected to this gain fiber is coated on an MMF-S105/125 fiber (Coherent, with core and cladding diameters of 105 μm and 125 μm, respectively, and NA of 0.22). To achieve low-loss connection between gain fiber and FDMs, high-performance FC/PC fiber connectors must be prepared at both ends of the double-clad $Pr^{3+}$-doped ZBLAN fiber. However, the fragile mechanical properties of fluoride fibers often lead to end-facet damage during conventional polishing processes, which limits the damage threshold and impedes high-power operation. To address this challenge, we developed a novel fluoride fiber end-facet processing technique. This method employs a commercial fiber cleaver (CT104+, Fujikura) for precise fiber cutting, followed by butt-coupling with other fiber components via ceramic ferrules. The approach not only minimizes end-facet damage but also enables angle-cut end facets, effectively suppressing Fresnel reflection-induced laser self-excitation effects at the other end of the gain fiber. The pump source is a multi-mode blue laser diode (LD) with a maximum continuous wave(CW) power of 12 W at 443 nm, coupled to the FDM ($M_1$) via a 7.5 mm focal length aspherical lens ($L_1$), and the FDM ($M_1$) is connected to the gain fiber. The other end of the gain fiber guides the fluorescence beam into the AOM through the collimator and then reflects to the gain fiber through the $M_2$ mirror at the rear end to form a closed resonator. The homemade FDM ($M_2$) and a free-space dichroic mirror construct the linear cavity feedback for red-light oscillation. All the mirrors ($M_1$, $M_2$) within the cavity were coated with the same $SiO_2/Ta_2O_5$ multilayer dielectric films, and their transmission spectrum in Fig. 1(h) exhibits a 95% high transmittance at 443 nm and a 92% high reflectivity at 635 nm. The visible spatial AOM with an RF operation frequency of 100 MHz can operate in the wide visible range of 530–640 nm. The AO medium measures $10 \times 16 \times 5$ $mm^3$, has a 16 mm light transmission length, and the maximum light aperture is 1.5 mm. To achieve stable active mode-locking operation, the AOM must be placed in the resonator, and the AOM must maintain a specific diffraction angle with the optical path in the cavity. The modulation frequency of the AOM was determined by the formula ($f = c/2nL$), where n is the refractive index of the gain fiber and L is the cavity length. This ensures precise matching between the modulation frequency and the cavity resonance, enabling stable mode-locking operation. To avoid additional insertion losses from external output couplers, the laser output was extracted solely through the first-order diffracted light of the AOM. The output coupling ratio was controlled by adjusting the duty cycle of the pulsed signal from the signal generator driving the AOM. Experimental observations revealed that a lower output coupling ratio significantly enhances the intracavity power density, facilitating more robust and stable mode-locking initiation. This approach eliminates the need for auxiliary components while maintaining precise control over the energy extraction efficiency. This design ensures efficient power extraction while maintaining the stability of the mode-locked state. The first-order diffraction efficiency at 635 nm is approximately 88%, and the insertion loss is 0.5 dB. Specifically, at 635 nm, the feedback of the entire resonator has a high reflectivity, and the output is only extracted by a free-space binary mirror ($M_3$) of the first-order diffractive light of AOM, with an output coupling ratio of approximately 8%.

As shown in Fig. 1(c), the orange AML laser uses a 5 cm $Pr^{3+}/Yb^{3+}$-doped ZBLAN fiber (Le Verre Fluoré, with core and cladding diameters of 3.5 μm and 125 μm, respectively, and NA of 0.16) as the gain fiber based on the structure of the red laser. Due to the strong absorption of this gain fiber at 443 nm, a shorter length is necessary, which results in

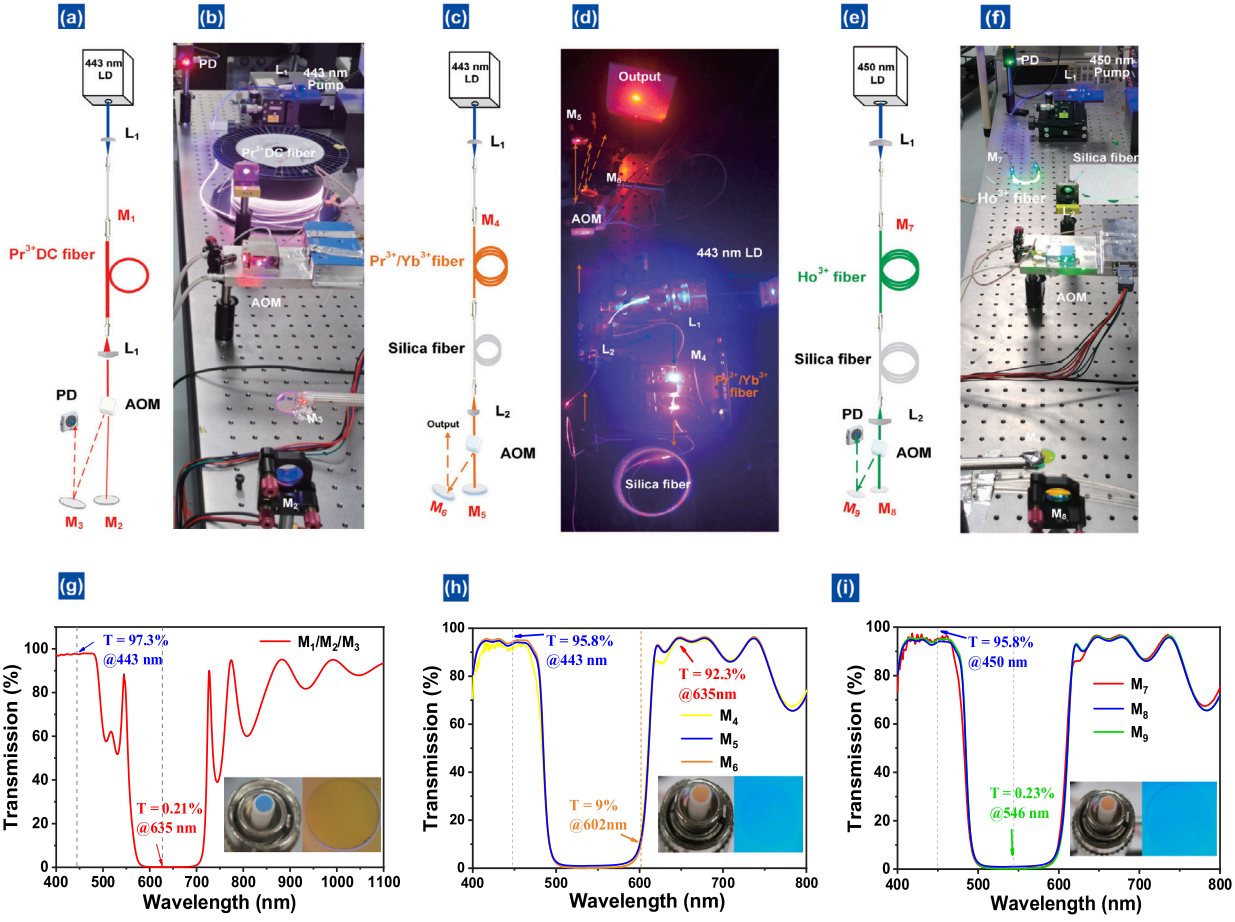


**Fig. 1.** (a, c, e) Schematics and (b, d, f) Photographs of the AML lasers based on AOM at 635 nm,602 nm and 546 nm. (g, h, i) The transmission spectra of the fiber dichroic mirrors ($M_1$, $M_4$, $M_7$) and the visible plane mirrors ($M_2$, $M_3$ $M_5$, $M_6$ $M_8$, $M_9$) Inset: Photograph and microscopic image of fiber dichroic mirror.

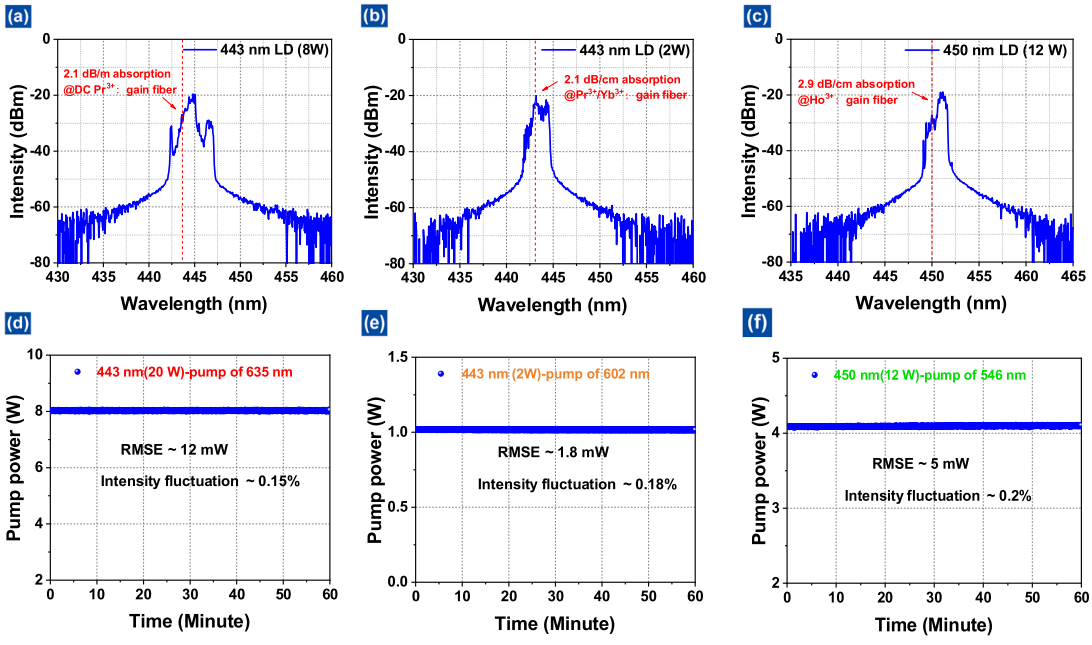


**Fig. 2.** (a–c) Pump spectrum and absorption coefficient corresponding to 635 nm, 602 nm and 546 nm AML fiber laser. (d–f) Pump source power stability corresponding to 635 nm, 602 nm and 546 nm AML fiber laser.

the connection of a 79 m extension fiber (630-HP fiber, with core and cladding diameters of 3.5 μm and 125 μm, respectively, and NA of 0.13) at the rear end of the gain fiber to adapt to the cavity length required by the maximum modulation frequency of the AOM at 602 nm. Fig. 1(h)

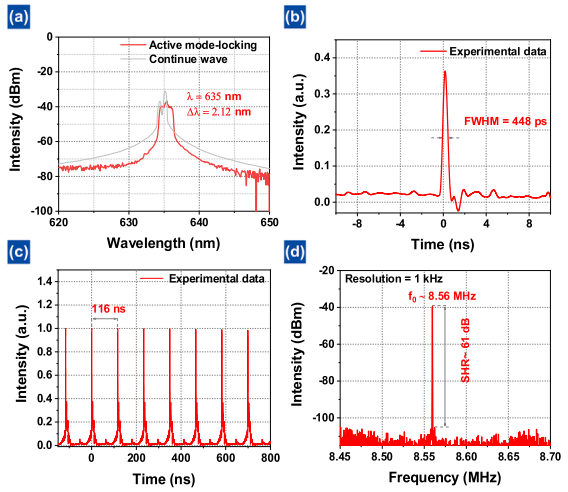


**Fig. 3.** Characteristics of the red AML pulse operation at 635 nm. (a) Output optical spectrum. (b) Single pulse. (c) The typical oscilloscope trace. (d) RF output spectra.

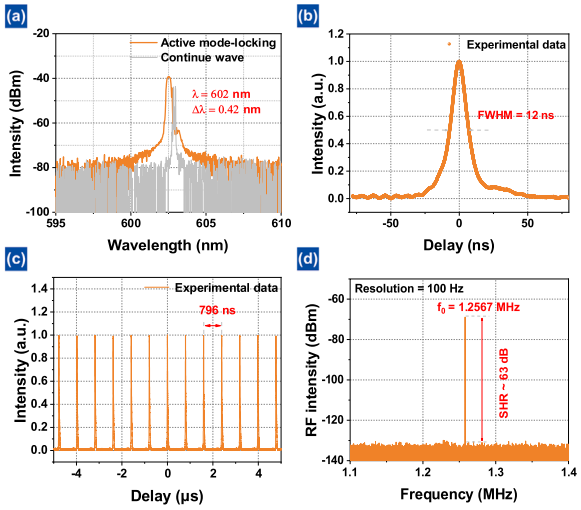


**Fig. 4.** Characteristics of the orange AML pulse operation at 602 nm. (a) Output optical spectrum. (b) Single pulse. (c) The typical oscilloscope trace. (d) RF output spectra.

shows the transmission spectrum of the mirrors of an orange resonator with a 95% high transmittance at 443 nm, a 92% high transmittance at 635 nm, and a 92% high reflectivity at 603 nm. Because red light (635 nm) has the largest emission cross section in $Pr^{3+}/Yb^{3+}$-doped ZBLAN fiber (i.e., the red gain is much stronger than that of orange light) and is very close to orange light (~30 nm), the homemade orange FDM ($M_4$) can suppress red self-excitation under high orange light gain. Due to the relatively weaker gain at 602 nm in the $Pr^{3+}/Yb^{3+}$-doped fiber, a stronger feedback (corresponding to a 3% output coupling ratio) was required to achieve optimal performance.

Similarly, the green AML fiber laser selects the $Ho^{3+}$-doped ZBLAN fiber (Le Verre Fluoré, with core and cladding diameters of 7.5 μm and 125 μm, respectively, and NA of 0.23) as the gain fiber and a 12 W 450 nm diode laser as the pump source in a similar structure shown in Fig. 1(f). A 24.6 m extension fiber (Corning, SMF 1950, with core and cladding diameters of 7 μm and 125 μm, respectively, and NA of 0.2) is inserted into the cavity to match the acousto-optic modulation at the maximum frequency in the green band. The transmission spectrum of the green resonator's mirrors ($M_7$, $M_8$) is shown in Fig. 1(i), with a transmittance of up to 95.8% at 450 nm and a high reflectivity of 99.77% at 546 nm. To achieve the best output characteristics, the output coupling ratio of the green AML fiber laser was set to 10%. This configuration ensures a balance between efficient energy extraction and the preservation of desirable mode-locked pulse properties. The output performance of visible AML fiber lasers in the spectral domain is characterized by a 350–1750 nm optical spectrum analyzer (AQ-6315E, Ando) with a 0.05 nm resolution. The pulse train and radio-frequency (RF) spectrum are recorded by a 12.5-GHz photodetector (ET-4000F, Electro-Optics Technology, Inc.) in conjunction with a 12-GHz, 40 GS/s oscilloscope (DSO81204 A, Agilent Infiniium) or an electrical spectrum analyzer (N9020 A, Agilent). The signal generator is the AFG31000(150 MHz) model from Tektronix. Power measurements are conducted using a 350 to 1100 nm optical power meter (S142C, Thorlabs, Inc.). Calibration certificates and related documentation can be accessed through the manufacturers' official websites. Therefore, we consider the performance of these devices to be reliable, and our experiments did not perform additional calibration of these instruments.

To ensure clarity in the experimental process, we conducted detailed tests on the pump sources for the three AML fiber lasers. For the red AML fiber laser, which utilizes a double-clad gain fiber, a 20 W fiber-coupled LD at 443 nm was employed as the pump source, with a center wavelength of 443.8 nm and an absorption coefficient of 2.1 dB/m for

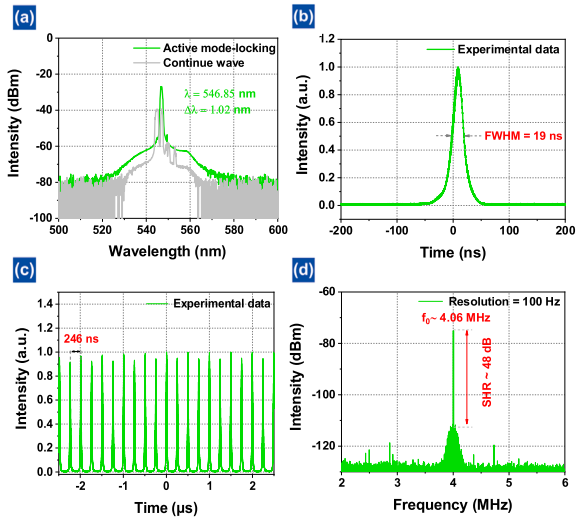


**Fig. 5.** Characteristics of the green AML pulse operation at 546 nm (a) Output optical spectrum. (b) Single pulse. (c) The typical oscilloscope trace. (d) RF output spectra.

double-clad $Pr^{3+}$-doped ZBLAN fiber (Fig. 2(a)). Pump source power stability was measured (Fig. 2(d)), and at the typical operating power of 8 W, the pump source exhibited a power fluctuation of 12 mW with a root-mean-square error (RMSE) of 0.15%. For the orange AML fiber laser, which employs a quasi-single-mode gain fiber, a high-beam-quality 2 W single-emitter LD at 443 nm was used as the pump source. The LD with a central wavelength of 443.5 nm and an absorption coefficient of 2.1 dB/cm for $Pr^{3+}/Yb^{3+}$-doped ZBLAN fiber, as shown in Fig. 2(b). We measured the pump source power stability, as depicted in Fig. 2(e). At the typical operating power of 1 W, the pump source demonstrated a power fluctuation of 1.8 mW, with an RMSE of 0.18%. For the green AML fiber laser, which utilizes a multimode single-clad gain fiber, a 12 W multi-emitter LD at 450 nm was selected as the pump source. The pump source has a center wavelength of 451 nm and an absorption coefficient of 2.9 dB/cm for $Ho^{3+}$-doped ZBLAN fiber, as shown in Fig. 2(c). We measured pump source power stability, as depicted in Fig. 2(f). At the typical operating power of 4 W, the pump source showed a power fluctuation of 5 mW, with an RMSE of 0.2%.

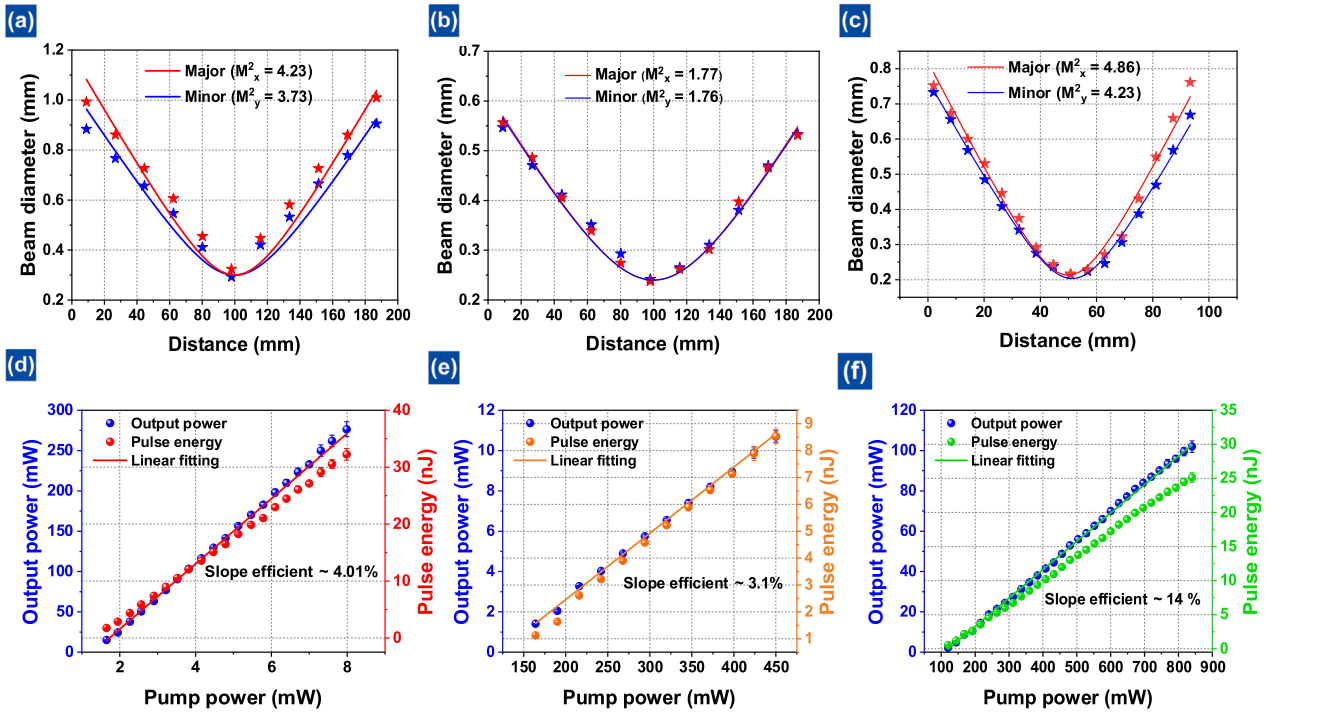


**Fig. 6.** (a–c) $M^2$ factors of the generated visible fiber laser beam corresponding to 635 nm, 602 nm and 546 nm. (d–f) Average output power and pulsed energy as a function of the pump power corresponding to 635 nm, 602 nm and 546 nm.

## 3. Results and discussion

The typical output parameters of the red AML fiber laser operating at a pump power of 6.5 W are presented in Fig. 3. As depicted in Fig. 3(a), the mode-locked optical spectrum has a 3-dB bandwidth of 2.12 nm and a center wavelength of 635.5 nm. We also provide the spectrum in the continuous wave state, showing unstable multi-wavelength lasing near the central wavelength. As shown in Fig. 3(b), the single pulse envelope has a symmetrical intensity profile resembling a Gaussian shape, and the pulse duration is 448 ps. The typical pulse train with a 116 ns pulse interval and consistent pulse intensity is displayed in Fig. 3(c). Furthermore, as illustrated in Fig. 3(d), the output RF spectrum has a signal-to-noise ratio of approximately 61 dB and a fundamental frequency of 8.56 MHz. To ensure the accuracy of the SNR measurements, all experiments were conducted in a professional optical laboratory with strict environmental controls. The laboratory is equipped with a 24-h air conditioning system to maintain a stable temperature (with fluctuations of less than 1 °C), and the optical setup was placed on a vibration-isolation platform (air-floating optical table) to eliminate mechanical vibrations.

Fig. 4 summarizes the typical characteristics of orange active mode locking operation at a pump power of 450.7 mW. As presented in Fig. 4(a), the laser center wavelength is 602.4 nm, and its 3 dB linewidth is 0.42 nm. The spectrum of orange light in the CW state also shows unstable multi-wavelength lasing. Fig. 4(b) provides the typical oscilloscope trace of the AML pulses. The single pulse envelope has a symmetrical Gaussian-like intensity profile with a FWHM of 12 ns. Unlike red picosecond active mode-locking lasers, orange active mode-locking pulses are on the order of nanoseconds due to the strong positive dispersion introduced by the 70 m extended fiber in the cavity. The pulse trains with a period of 796 ns have a pulse-intensity fluctuation as low as 5%. As shown in Fig. 4(c), the fundamental RF peak (i.e., pulse repetition rate) is 1.2567 MHz, which agrees with the pulse period of 796 ns. The RF signal-to-noise ratio is more than 62 dB, comparable to those of passively mode-locked visible fiber lasers. These results indicate that the orange AML laser is stable and could be suitable for practical applications.

We experimentally investigated the characteristics of green AML fiber lasers at 546 nm. Fig. 5(a) displays the green output spectra with the 3-dB linewidth of 1.02 nm and the center wavelength of 546.85 nm. The single mode locked pulse envelope is depicted in Fig. 5(b). The pulse has a length of 19 ns and a Gaussian-like intensity profile. A period of 246 ns corresponds to 4.06 MHz and a pulse-to-pulse variability of 6%, as shown in Fig. 5(c). Fig. 5(d) displays the RF spectrum of the output. With an RF signal-to-noise ratio greater than 48 dB and a fundamental frequency peak at 4.06 MHz, the pulse period of 246 ns is stable. Low noise near the fundamental frequency is observed, which may result from the large spot emitted by the $Ho^{3+}$-doped ZBLAN fiber and the partial green light that exceeds the size of the acousto-optic crystal and remains unmodulated.

Additionally, we measured the beam quality and output powers of the three AML fiber lasers in red, orange, and green. The $M^2$ factors of the generated visible fiber laser beam were measured by a beam quality analyzer (WinCamD-UCD12, DataRay), and the measurement results are shown in Fig. 6(a–c). The measured $M^2$ x;y parameters of the red AML laser are 4.15 and 3.44, respectively, indicating that the red DC $Pr^{3+}$-doped fluoride fiber laser operates in a multi-transverse mode. According to the measurement results of the orange AML fiber laser shown in Fig. 6(b), the measured $M^2$ x;y values of the major and minor axes are 2.06 and 1.69, respectively. Therefore, the output laser beam has a few-mode output in the $Pr^{3+}/Yb^{3+}$ -doped ZBLAN fiber laser. Since the $Ho^{3+}$-doped ZBLAN fiber in the green AML fiber laser is a multi-mode fiber, $M^2$ x;y parameters of 4.86 and 4.23 are measured, as shown in Fig. 6(c). Fig. 6(d) presents the laser output power of the red AML fiber laser as a function of the injected pump power. Under the repetition rate of 8.56 MHz, the threshold of the red AML laser was ~1.6 W. A maximum output power of 275 mW was obtained at a pump power of 8 W, corresponding to a maximum pulse energy of 32 nJ, and the slope efficiency is 4.01%. Through repeated measurements of the power data, we conducted an error analysis and observed that the red AML fiber laser exhibits power fluctuations (approximately 10 mW) when operating at its maximum output power. These fluctuations are attributed to minor thermal damage on the end faces of the fluoride

**Table 1**
Output performance of visible pulsed fiber lasers based on active device modulation.

| Theory | Device | ZBLAN fiber | Wavelength (nm) | Power (mW) | Frequency (MHz) | Pulse width (ns) | Year |
|---|---|---|---|---|---|---|---|
| Active mode-locking | PFOM | $Pr^{3+}/Yb^{3+}$ | 635 | 3 | 239 | 0.55 | 2000 [23] |
| | AOM | DC $Pr^{3+}$ | 635 | 275 | 8.56 | 0.44 | This work |
| | AOM | $Pr^{3+}/Yb^{3+}$ | 602 | 11 | 1.25 | 12 | This work |
| | AOM | $Ho^{3+}$ | 545 | 102 | 4.06 | 19 | This work |
| Cavity-dumping | AO Q-switch | $Ho^{3+}$ | 546 | 310 | 0.0001 | 116 | 2023 [29] |
| Frequency-shift-feedback | AOM | DC $Pr^{3+}$ | 635 | 78 | 31.8 | 0.045 | 2024 [30] |

fiber, which occurs under extreme power conditions. Notably, such fluctuations are not significant when the laser operates within safe power ranges. In Fig. 6(e), compared with the higher output power of the red AML laser, the gain fiber of the orange light laser is a few-mode fiber. As a result, the output power of orange light is 11 mW, corresponding to a pulse energy of 8.7 nJ at a repetition rate of 1.256 MHz, with a slope efficiency of 3.1%. For the orange AML fiber laser, power fluctuations near the maximum output power were observed to be around 1 mW. The relatively low slope efficiency of the orange mode-locked fiber laser is primarily attributed to the high insertion loss (~27%) at the interfaces of the $Pr^{3+}/Yb^{3+}$-doped ZBLAN fiber. This issue arises from the small core diameter of the gain fiber and its poor concentricity during fabrication, which leads to core misalignment. This problem can be mitigated by utilizing specially designed eccentric passive fibers for splicing. Additionally, the intrinsic loss of the 79 m 630 HP fiber at 602 nm is relatively high (~6.3%), further reducing the output efficiency. In future work, replacing the 630 HP fiber with passive ZBLAN fiber is expected to address these challenges and improve overall performance. Fig. 6(f) shows the average output power and pulse energy as a function of the pump power in a green AML fiber laser. Under a pump power of 832 mW, the green AML fiber laser generated a maximum output power of 102 mW, with a pulse energy of 25 nJ and a slope efficiency of 14%. For the green AML fiber laser, power fluctuations near the maximum output power were observed to be around 3 mW. For the green mode-locked laser, the splicing loss is relatively low due to the larger core diameter and better concentricity of the $Ho^{3+}$-doped ZBLAN fiber. At the same time, the 24.6 m SMF 1950 fiber contributed 0.04 dB, causing only 1.0% power propagation loss. Indicating that quantum defect and AOM insertion loss dominated its efficiency limitations. In summary, visible AML fiber lasers operating at 635 nm and 546 nm with multi-mode gain fibers can produce output powers exceeding 100 mW. However, this high output power is achieved at the expense of beam quality. The orange AML laser has achieved beam quality close to that of a single-mode laser, but its output power needs to be further improved. In the future, visible AML pulses with higher performance can be obtained by optimizing beam collimation and using acousto-optic crystals with larger optical apertures.

To better illustrate the advantages of our AML fiber laser over other visible pulsed lasers based on active modulation devices previously reported, Table 1 compares the output performance of current visible pulsed fiber lasers modulated by active devices. It is worth noting that visible actively Q-switched fiber lasers are also achievable, but they typically suffer from limitations such as wide pulse durations (even in the μs range) and narrow repetition rate ranges (in the kHz range), resulting in less significant output performance advantages and consequently fewer reports. In this study, we report three visible AML fiber lasers operating at red (635 nm), orange (602 nm), and green (546 nm) wavelengths. From Table 1, the following observations can be made: (1) The only prior report on visible-wavelength active mode-locking technology dates back to over two decades ago, where researchers achieved 3 mW of 635 nm pulses with a pulse width of 550 ps using an all-fiber phase modulator (PFOM) in $Pr^{3+}/Yb^{3+}$-doped ZBLAN fiber, laying the foundation for active mode-locking. However, due to the use of a custom few-mode fiber phase modulator, the output power was extremely low, making it difficult to apply to multimode gain fibers and limiting its potential for wavelength extension. (2) An AOM was employed as the active mode-locking device in conjunction with double-clad $Pr^{3+}$-doped ZBLAN fiber, enabling high-power (275 mW) red AML pulses. This approach increased the output power by two orders of magnitude while achieving a narrower pulse width (448 ps). (3) This work proposes a universal AOM-based active mode-locking architecture for the visible wavelength range. Utilizing $Pr^{3+}/Yb^{3+}$-doped ZBLAN fiber and multimode $Ho^{3+}$-doped ZBLAN fiber, we have also demonstrated, for the first time, orange and green AML pulses, filling a critical gap in this field. (4) Other visible-wavelength pulsed lasers based on active modulators include cavity-dumped lasers, which typically operate at very low repetition rates to achieve high pulse energy but often exhibit broad pulse widths (116 ns). Additionally, frequency-shifted feedback ultrafast fiber lasers usually operate at low power and high repetition rates (37.1 MHz) to generate ultrafast pulses. However, the stability requirements for mode-locking in such frequency-shifted feedback systems are significantly higher than those for AML fiber lasers. Therefore, visible AML fiber lasers, with their relatively narrow pulse widths, simple structure, and strong stability, are better suited for diverse application scenarios under varying environmental conditions.

Despite these advancements, our work has two main limitations that need to be addressed in future studies: (1) The introduction of a relatively long passive fiber within the cavity leads to pulse broadening in both the green and orange wavelengths due to dispersion. In future work, we aim to address this by optimizing the length of the passive fiber and fine-tuning the modulation frequency of the AOM to further compress the pulse width. (2) The output power of the orange laser is lower than expected, primarily due to higher cavity losses caused by the imperfect concentricity of the few-mode gain fiber. To overcome this, we propose developing advanced splicing techniques for fluoride fibers, which could significantly reduce cavity losses and improve output power.

## 4. Conclusion

In summary, we demonstrated three AML fiber lasers of different wavelengths by leveraging the visible down-conversion gain of three rare-earth-ion-doped ZBLAN fibers and the intensity modulation of AOM, providing a platform for the study of visible AML characteristics. Three 635 nm/602 nm/546 nm AML lasers with pulse durations of 448 ps/12 ns/19 ns and maximum average powers of 275 mW/11 mW/102 mW were obtained. Through the analysis of their performance parameters, significant optimization potential was identified, and an optimization scheme was proposed. The system broke the stagnation of AML technology in the visible range for more than twenty years. For the first time, active mode-locking pulses were achieved in orange and green wavelengths, while the output performance in red surpassed that of similar products in previous studies. This work paves the way for promising applications of visible AML lasers, such as visible fiber communications and ultra-wideband signal processing.

## CRediT authorship contribution statement

**Tianran Li:** Writing – original draft, Methodology, Investigation, Formal analysis, Data curation, Conceptualization. **Shuo Zhang:** Software, Methodology, Data curation. **Jinliang Yuan:** Resources, Data

curation. **Yikun Bu:** Supervision, Software, Resources. **Mingjia Shangguan:** Supervision, Resources. **Zhengqian Luo:** Writing – review & editing, Writing – original draft, Supervision, Software, Resources, Methodology, Funding acquisition, Conceptualization.

## Declaration of competing interest

The authors declare no conflicts of interest.

## Data availability

Data will be made available on request.

## References


[1] Hassan M. Oubei, Jose R. Duran, Bilal Janjua, Huai Yung Wang, Cheng Ting Tsai, 4.8 Gbit/s 16-QAM-OFDM transmission based on compact 450-nm laser for underwater wireless optical communication, Opt. Express 23 (2015) 23302–23309.

[2] Martin E. Fermann, Ingmar Hartl, Ultrafast fibre lasers, Nat. Photonics 7 (11) (2013) 868–874.

[3] Mangirdas Malinauskas, Albertas Zukauskas, Satoshi Hasegawa, Yoshio Hayasaki, Saulius Juodkazis, Ultrafast laser processing of materials: from science to industry, Light.: Sci. Appl. 5 (8) (2016) e16133.

[4] Koji Sugioka, Ya Cheng, Ultrafast lasers-reliable tools for advanced materials processing, Light.: Sci. Appl. 3 (4) (2014) e149.

[5] Robin Mevert, Yuliya Binhammer, Christian Dietrich, Luise Beichert, Thomas Binhammer, José Cardoso de Andrade, Jintao Fan, Uwe Morgner Morgner, Widely tunable, high-power, femtosecond noncollinear optical parametric oscillator in the visible spectral range, Photonics Res. 9 (11) (2021) 1715.

[6] Zhipeng Dong, Hang Wang, Wencheng Jia, Jinhai Zou, Zhengqian Luo, All-polarization-maintaining, mode-locked 488 nm picosecond laser, IEEE Photonics Technol. Lett. 35 (6) (2023) 283–286.

[7] D. Taverner, P. Britton, P.G.R. Smith, D.J. Richardson, G.W. Ross, D.C. Hanna, Highly efficient second-harmonic and sum-frequency generation of nanosecond pulses in a cascaded erbium-doped fiber periodically poled lithium niobate source, Opt. Lett. 23 (3) (1998) 162–164.

[8] Ortwin Hellmig, Stefan Salewski, Arnold Stark, Jörg Schwenke, Peter E. Toschek, Klaus Sengstock, Valery M. Baev, Multicolor diode-pumped upconversion fiber laser, Opt. Lett. 35 (13) (2010) 2263–2265.

[9] H. Okamoto, K. Kasuga, Y. Kubota, Efficient 521 nm all-fiber laser: splicing $Pr^{3+}$-doped ZBLAN fiber to end-coated silica fiber, Opt. Lett. 36 (8) (2011) 1470.

[10] Jun Nakanishi, Yuya Horiuchi, Tsuyoshi Yamada, Osamu Ishii, Masaaki Yamazaki, Minoru Yoshida, Yasushi Fujimoto, High-power direct green laser oscillation of 598 mW in $Pr^{3+}$-doped waterproof fluoroaluminate glass fiber excited by two-polarization-combined GaN laser diodes, Opt. Lett. 36 (10) (2011) 1836–1838.

[11] Jinhai Zou, Chuchu Dong, Hongjian Wang, Tuanjie Du, Zhengqian Luo, Towards visible-wavelength passively mode-locked lasers in all-fibre format, Light.: Sci. Appl. 9 (1) (2020).

[12] Saiyu Luo, Han Gu, Xiao Tang, Xiang Geng, Li Li, Zhiping Cai, High-power yellow DSR pulses generated from a mode-locked Dy:ZBLAN fiber laser, Opt. Lett. 47 (5) (2022) 1157–1160.

[13] Saiyu Luo, Xiao Tang, Xiang Geng, Han Gu, Li Li, Zhiping Cai, Ultrafast true-green Ho:ZBLAN fiber laser inspired the $TD_3$ AI, Opt. Lett. 47 (5) (2022) 1157–1160.

[14] Marie-Pier Lord, Michel Olivier, Martin Bernier, Réal Vallée, Visible femtosecond fiber laser, Opt. Lett. 48 (14) (2023) 3709–3712.

[15] Qiujun Ruan, Xiaosheng Xiao, Jinhai Zou, Hang Wang, Shuzheng Fan, Tianran Li, Jin Li, Zhipeng Dong, Zhiping Cai, Zhengqian Luo, Visible-wavelength spatiotemporal mode-locked fiber laser delivering 9 ps, 4 nJ pulses at 635 nm, Laser Photonics Rev. 16 (7) (2023) 2100678.

[16] Jinhai Zou, Qiujun Ruan, Tingting Chen, Hang Wang, Luming Song, Yikun Bu, Zhengqian Luo, 635 nm femtosecond fiber laser oscillator and amplifier, Adv. Photonics Nexus 3 (2) (2024) 026004.

[17] Tengfei Dai, Youpeng Su, Yuanyuan Li, Tianyi Lu, Hongxu Li, Jianhua Chang, Actively mode-locked fiber laser with graphene fiber modulator, J. Lightwave Technol. (17) (2024) 42.

[18] Yali Zhang, Juncheng Li, Chengzhen Meng, Shouhai Li, Zhen Zeng, Lingjie Zhang, Zhiyao Zhang, Shangjian Zhang, Yong Liu, Actively mode-locked modulator-free optoelectronic oscillator for multi-functional microwave pulse generation, J. Lightwave Technol. 42 (19) (2024) 7.

[19] T. Xie, W. Dai, S. Zheng, H. Wang, M. Wu, C. Huang, H. Fu, A flexibly frequency switchable active mode-locking optoelectronic oscillator with supermode noise suppression, Opt. Laser Technol. 163 (2023) 109354.

[20] Peng Lin, Tianshu Wang, Wanzhuo Ma, Junda Chen, Ziqi Jiang, Ce Yu, 2-μm free-space data transmission based on an actively mode-locked holmium-doped fiber laser, IEEE Photonics Technol. Lett. 32 (5) (2020) 223–226.

[21] Wanzhuo Ma, Tianshu Wang, Furen Wang, Desheng Zhao, Runmin Liu, Jing Zhang, Huilin Jiang, 2.07-μm, 10-GHz repetition rate, multi-wavelength actively mode-locked fiber laser, IEEE Photonics Technol. Lett. 31 (3) (2019) 242–245.

[22] Masataka Nakazawa, Masato Yoshida, Toshihiko Hirooka, The nyquist laser, Optica 1 (1) (2014) 15.

[23] D.M. Costantini, H.G. Limberger, T. Lasser, C.A.P. Muller, H. Zellmer, P. Riedel, A. Tünnermann, Actively mode-locked visible upconversion fiber laser, Opt. Lett. 25 (19) (2000) 1445–1447.

[24] Ido Cooperstein, Efrat Shukrun, Ofir Press, Alexander Kamyshny, Shlomo Magdassi, Additive manufacturing of transparent silica glass from solutions, ACS Appl. Mater. Interfaces 10 (22) (2018) 18879–18885.

[25] Shengjie Ding, Shixun Dai, Zhongchao Wu, Zhenfei Cao, Lulu Xu, Min Wang, High-performance acousto-optic modulator based on environmentally favorable $Ge_{20}Sb_{15}Se_{65}$ chalcogenide glass, Ceram. Int. 47 (21) (2021) 30343–30348.

[26] Zenghua Xu, Shixun Dai, Chengcheng Liu, Zhongchao Wu, Lulu Xu, Investigation of the Ga-SB-S chalcogenide glass with low thermo-optic coefficient as an acousto-optic material, Ceram. Int. 48 (15) (2022) 21663–21670.

[27] Feifei Guo, Fuai Hu, Lijuan Chen, Xutang Tao, Zeliang Gao, High-quality acousto-optic modulators with high diffraction efficiency, polarization extinction ratio, and small insertion loss based on a novel $BaO–TeO_2–WO_3$ glass, Adv. Mater. 36 (8) (2024) 2308079.

[28] Jinhai Zou, Jinfen Hong, Zhuang Zhao, Qingyuan Li, Qiujun Ruan, Hang Wang, Yikun Bu, Xianchao Guan, Min Zhou, Zhiyong Feng, 3.6W compact all-fiber $Pr^{3+}$-doped green laser at 521nm, Adv. Photonics 4 (5) (2022) 9.

[29] Tianran Li, Ziyu Wang, Jinhai Zou, Jinfen Hong, Qiujun Ruan, Hang Wang, Zhipeng Dong, Zhengqian Luo, Direct generation of 3.17 mJ green pulses in a cavity-dumped $Ho^{3+}$-doped fiber laser at 543 nm, Photonics Res. 11 (3) (2023) 413–419.

[30] Tianran Li, Lu Huang, FeiFei Guo, Jingbin Lan, Lan Lan, Yikun Bu, Zeliang Gao, Zhengqian Luo, Ultrafast visible fiber laser mode-locked by frequency-shifted feedback of an $\alpha$-$BaTeMo_2O_9$ crystal acousto-optic modulator, Opt. Lett. 49 (22) (2024) 6357–6360.